P2M.3

WRF MODEL SIMULATIONS OF A QUASI-STATIONARY, EXTREME-RAIN-PRODUCING MESOSCALE CONVECTIVE SYSTEM

Russ S. Schumacher* and Richard H. Johnson
Department of Atmospheric Science, Colorado State University, Fort Collins, Colorado

1. INTRODUCTION

Extreme rainfall is responsible for a variety of societal impacts, including flash flooding that can lead to damage, injury, and death. In the United States, flash flooding is responsible for more fatalities than any other convective storm-related phenomenon, including tornadoes, hurricanes, and lightning (NOAA 2005). Despite the great need for accurate forecasts and warnings of extreme rainfall that can produce flash flooding, the prediction of warm-season heavy precipitation continues to be one of the most difficult challenges in operational forecasting (Fritsch and Carbone 2004).

In an attempt to understand more about how these extreme-rain-producing weather systems are organized and the conditions in which they occur, Schumacher and Johnson (2005, hereafter SJ05) examined radar data and other observations for 116 extreme rain events in the eastern two-thirds of the United States over a three-year period. Among the types of mesoscale convective systems (MCSs) that commonly produce extreme rainfall, they identified one that may present significant forecast challenges, which they termed the "backbuilding/quasi-stationary" type (BB, Fig. 1). BB MCSs occur when convective cells repeatedly form upstream of their predecessors and pass over a particular area, leading to large local rainfall totals. They were found to occur in environments characterized by weak synoptic forcing, with storm-generated outflow boundaries often providing the lifting for repeated cell development.

In this study, one of the BB MCSs identified by SJ05 will be examined in further detail using the Weather Research and Forecasting (WRF) model. This MCS, which produced rainfall amounts of up to 309 mm (12.2 in) and record flooding in Missouri on 6–7 May 2000, was characterized by an area of convection that remained quasi-stationary for approximately 6 h. The purpose of this study will be twofold: to determine the utility of the WRF model for simulating prolonged heavy-rain-producing convection, and to better understand the processes that are responsible for initiating, organizing, and maintaining such convection. Both of these purposes are focused on the goal of improving forecasts of extreme-rain-producing convective systems.

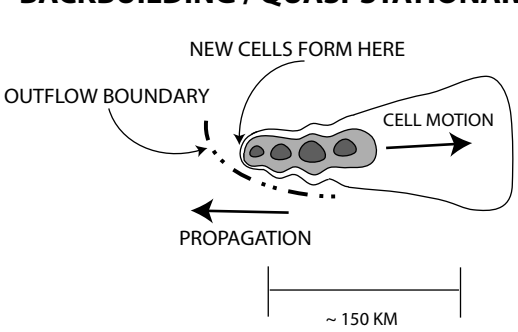

Figure 1: Schematic diagram of the radar-observed features of the BB pattern of extreme-rain-producing MCSs. Contours (and shading) represent approximate radar reflectivity values of 20, 40, and 50 dBZ. The dash-dot line represents an outflow boundary; such boundaries were observed in many of the BB MCS cases. The length scale at the bottom is approximate and can vary substantially for BB systems depending on the number of mature convective cells present at a given time. From Schumacher and Johnson (2005).

2. DESCRIPTION OF THE EVENT

During the evening and overnight hours of 6–7 May 2000 a small area of quasi-stationary convection produced a remarkable amount of rain over several counties just to the southwest of the St. Louis, Missouri metropolitan area (Fig. 2). The highest rainfall total reported at a National Weather Service rain gauge was 309 mm (12.15 in) at Union, MO, with unofficial reports of 406 mm (16 in) nearby (Glass et al. 2001). Consistent with past studies of

*Corresponding author address: Russ Schumacher, Department of Atmospheric Science, Colorado State University, Fort Collins, CO 80523-1371; rschumac@atmos.colostate.edu

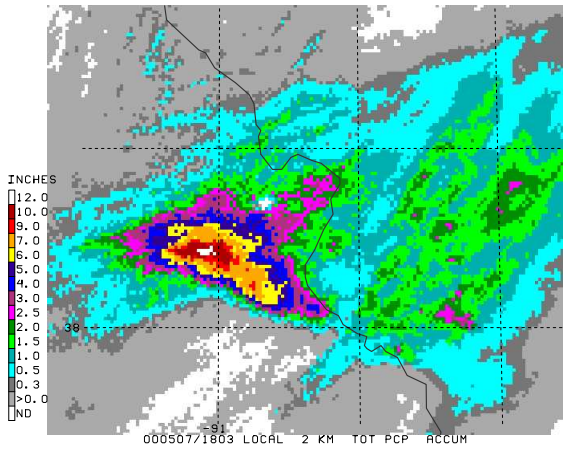

Figure 2: Estimated total precipitation (inches) from the KLSX WSR-88D for the period 0000–1803 UTC 7 May 2000. The thick line in the center of the figure is the border between Missouri and Illinois. Latitude and longitude lines are shown every 1°.

heavy rain environments (e.g., Maddox et al. 1979), there was high relative humidity in east-central Missouri as well as a 40-kt low-level jet from the southwest. However, in contrast to other observed extreme rainfall environments, there was relatively little instability and there were no apparent surface boundaries present prior to the onset of deep convection (not shown). A mesoscale convective vortex (MCV), evident in both the 500-hPa analysis and infrared satellite data, likely played a key role in initiating and maintaining the convection in this event. Convection developed around 0200 UTC and formed into a mesoscale area of deep convection that remained nearly stationary through 1200 UTC (Fig. 3). Only a very weak cold pool and outflow boundary developed as a result of the convection. For more observational details of this event, the reader is directed to the case study by Glass et al. (2001).

3. MODEL CONFIGURATION

The simulations presented herein were produced using version 2.0.3.1 of the advanced research WRF model (details available online at wrf-model.org). Simulations were carried out for the 24-h period 0000 UTC 7 May to 0000 UTC 8 May 2000 with a nested grid as shown in Fig. 4. The horizontal grid spacing was 9 km on the outer grid and 3 km on the inner grid, with 39 levels in the vertical. Cumulus convection was parameterized using the Kain-Fritsch scheme on domain 1, while convection was explicitly resolved on domain 2. Other details of the

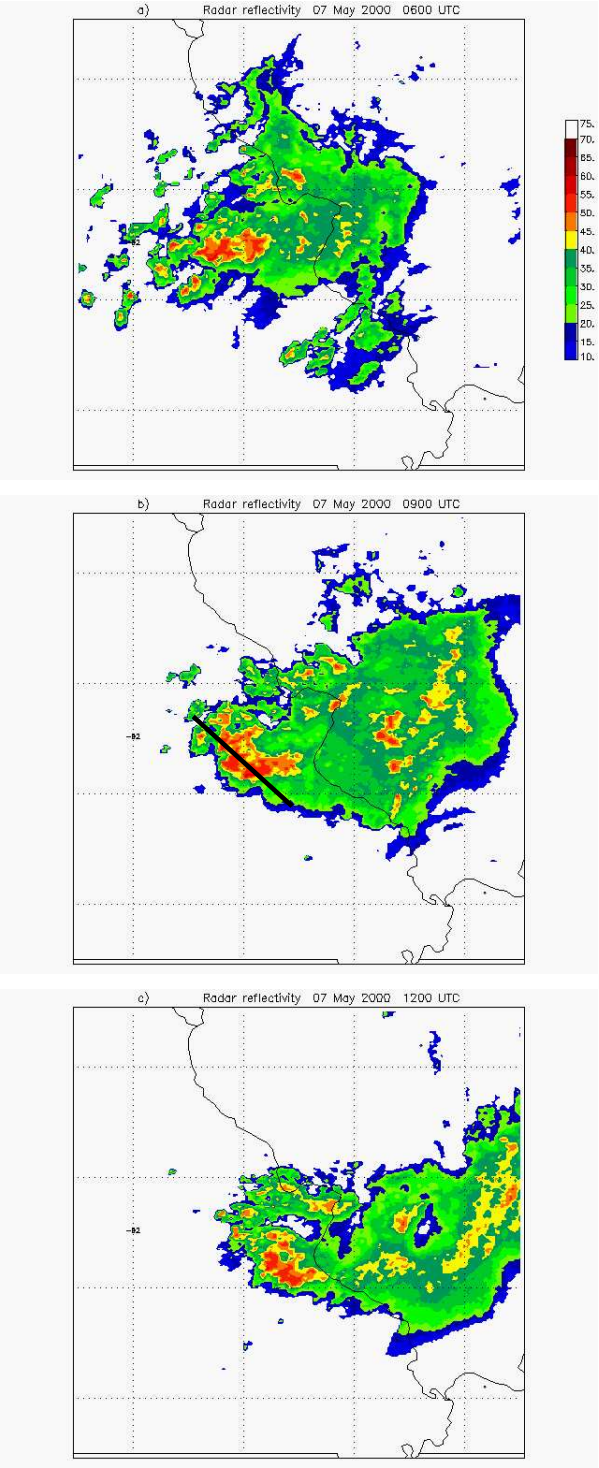

Figure 3: Composite radar reflectivity (dBZ) at (a) 0600, (b) 0900, and (c) 1200 UTC 7 May 2000. The thick line in panel (b) will be used for a cross section in Fig. 7.

Table 1: Design of WRF version 2.0.3.1 numerical model experiment. Multiple entries indicate different configurations for domains 1 and 2. See Fig. 4 for domain locations. Technical descriptions of these parameterizations are available online at wrf-model.org.

Horizontal grid spacing	9.0 km, 3.0 km
Vertical levels	39, 39
Initial conditions	40-km Eta
Boundary conditions	40-km Eta
Cumulus convection	Kain-Fritsch, explicit
Boundary layer	Yonsei University
Surface layer	Monin-Obukhov
Microphysics	Purdue Lin
Land surface	Noah
Turbulence	2D Smagorinsky
Shortwave radiation	Dudhia
Longwave radiation	Rapid radiative transfer

model configuration are shown in Table 1. The suite of parameterizations was chosen to resemble those used for real-time forecasts at the National Center for Atmospheric Research during the summers of 2003–2005. As such, this model configuration is similar to one that has demonstrated some success in near-real-time applications. However, given that the model initialization time is only a few hours before the onjset of convection in this study, the results presented herein should probably be considered a "simulation" rather than a "forecast" that could have been utilized in real-time.

4. RESULTS

4.1 *Overall structure of convection and precipitation*

The model successfully produces a backbuilding/quasi-stationary MCS which replicates many of the features of the observed system (Fig. 5). The model also succeds in producing a region of extreme rainfall amounts, the location and distribution of which is also remarkably similar to the observed rainfall (Fig. 6). The model underestimates the total rainfall amount; the maximum simulated rainfall is 257.6 mm, which is somewhat less than the observed maximum of 309 mm. However, given the challenges of predicting ground-accumulated rainfall when using microphysical parameterizations (e.g., Gilmore et al. 2004) and the remarkable amount of rain that fell in this event, this can probably be considered a successful result. While the convective region of the MCS is well-represented in the simulation, the model does not create the region of stratiform rain (with embedded convection) that extends eastward into Illinois in the observations.

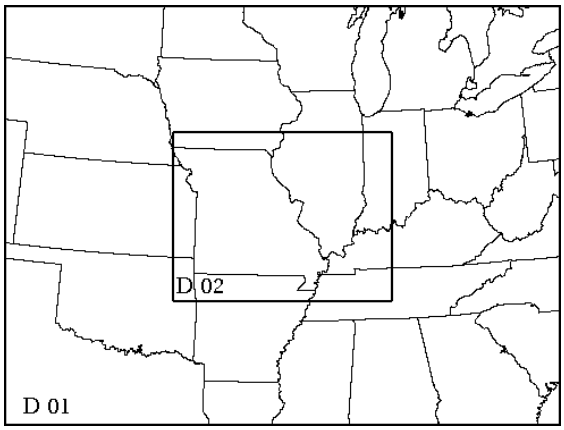

Figure 4: Location of model domains 1 and 2.

When observed in the vertical, the model is also fairly accurate in replicating the convective structure of this system. In the observations, a cross-section through the region of active convection demonstrates the backbuilding nature of this MCS (Fig. 7). There are two primary cells at 0907 UTC, with both bringing the 40-dBZ contour up to approximately 9 km. The southeastern cell (cell 1) has passed its mature phase and is decreasing in intensity, while the cell 2 (to the northwest of cell 1) is still intensifying and has a maximum in reflectivity extending from approximately 2 to 5 km. Two new cells, which will eventually intensify and mature, are beginning to organize to the left of the mature cells in the cross-section. The model results are quite similar, with the simulated 40-dbZ contour also reaching up to approximately 9 km, and the active cells having maximum reflectivities of 50–55 dBZ (Fig. 8). The observed backbuilding behavior in the observations is also represented in the simulation. As time progresses from panel (a) to panel (c) in Fig. 8, the eastern cell (cell 1) decays while the western cell (cell 2) strengthens. By 0930 UTC (Fig. 8c), the weak cell that had appeared on the very left edge (cell 3) of the figure has begun to intensify. The size of the cells appears to correspond well with the observations, though the distance between the simulated convective cells appears to be somewhat greater than observed. The cells appear to be, on average, around 10 km across, which is not a scale that is well-resolved with the current model configuration (i.e., the cells are only about 3 times as long as the model grid spacing). However, preliminary results with grid spacing of 1 km also show cells with similar size and spacing, suggesting that the

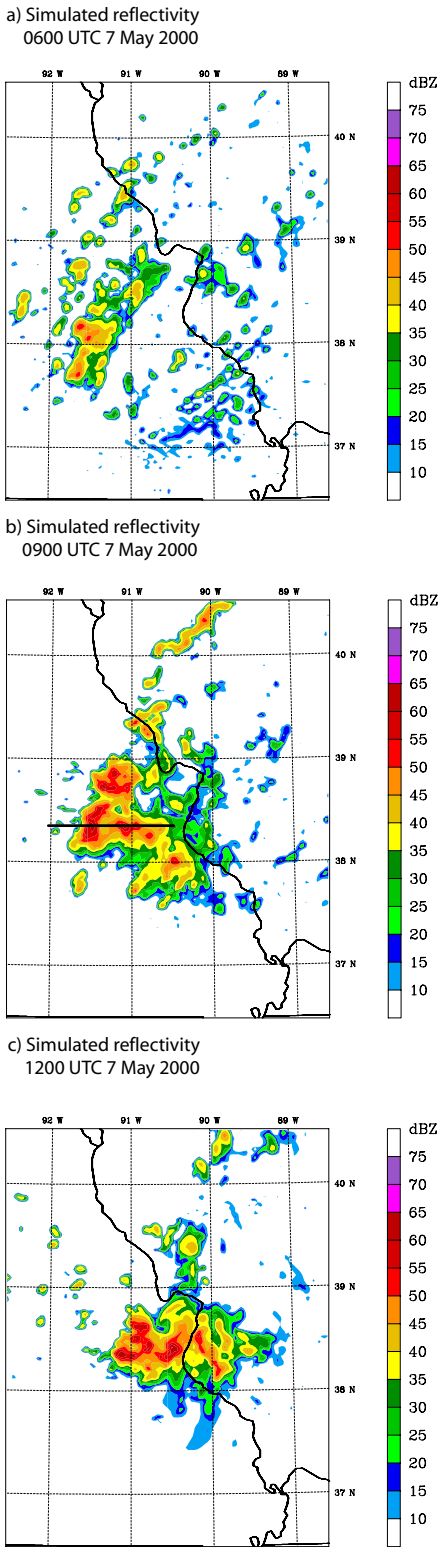

Figure 5: Simulated composite reflectivity (dBZ) on domain 3 at (a) 0600, (b) 0900, and (c) 1200 UTC 7 May 2000. The portion of the domain shown is the same as that shown in Fig 3 for comparison. The thick line in panel (b) will be used for a cross section in Fig. 8.

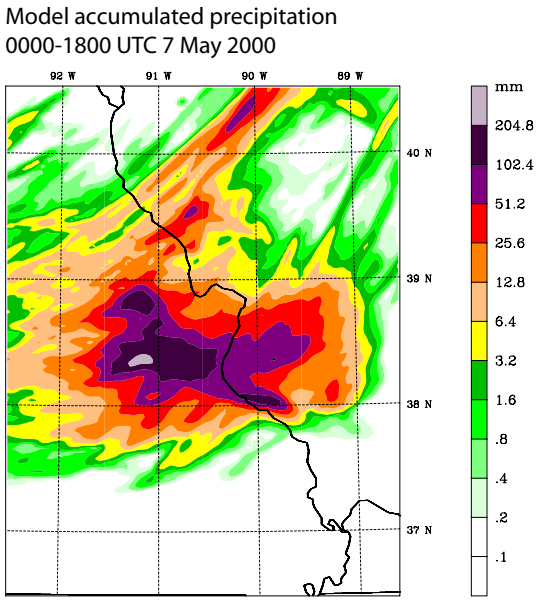

Figure 6: Model accumulated precipitation (mm) on domain 3 for the period 0000–1800 UTC 7 May 2000. For comparison with Fig. 2, recall that 1 in $\approx$ 25.4 mm, so the 102.4 mm (black) contour is approximately equal to the 4 in (blue) contour in Fig. 2.

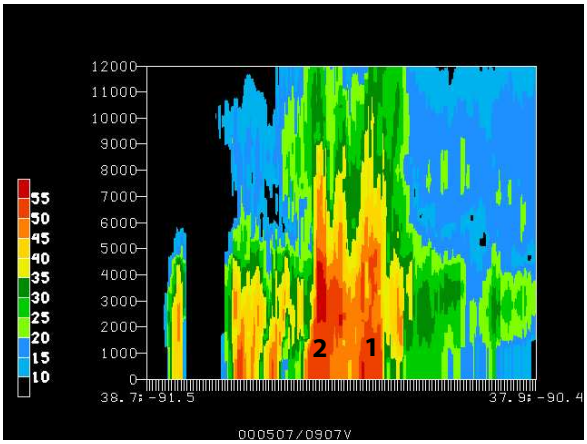

Figure 7: Reflectivity cross-section from the KLSX radar at 0907 UTC 7 May through the line noted in Fig. 3b. The scale on the vertical axis is km. Each tick mark on the horizontal axis is approximately 1 km; the span of the horizontal axis is approximately 131 km. Numbers refer to individual convective cells discussed in text.

convection represented at 3-km spacing does have some value. Again, while the model appears to accurately represent the convection, it does not create the region of 10–20 dBZ reflectivity aloft that is seen in the observations. This lack of hydrometeors aloft from the microphysics scheme helps to explain the model's failure to produce a region of stratiform rain downstream.

4.2 *Mesoscale convective vortex and moist absolute instability*

As mentioned above, at the time of model initialization an MCV existed over central Missouri, near the region where the heavy rain would later fall. This vortex was captured in the initial model analysis on domain 2 (Fig. 9). As illustrated by Trier and Davis (2002) and others, balanced motions that result from the presence of an MCV in vertical wind shear can lead to persistent convection directly beneath or just downshear of the vortex center. Additionally, Trier et al. (2000) show that the upward displacements that occur from this effect can destabilize the atmosphere by lifting initially moist and conditionally unstable layers to saturation. This can result moist absolutely unstable layers (MAULs, Bryan and Fritsch 2000). The model results from this case support these previous findings, with the heaviest rainfall occurring just downshear of the midlevel vortex center.

A model sounding from a point just west of the active convection (i.e., in the region where new cells are forming) at 1000 UTC shows the presence of a MAUL from approximately 775 hPa to 640 hPa (Fig. 10). Though there is relatively little convective available potential energy (CAPE) in this sounding (299 J kg^{-1}), there is also very little convective inhibition (CIN, -32 J kg^{-1}). The center of the midlevel MCV is immediately northwest of the convection at this time, and the hodograph plotted in the upper left of Fig. 10 illustrates that the low-level shear vector points toward the southeast in this region. Trajectories (not shown) on paths through the inflow region also show vertical displacements that are likely due to upward motions associated with the MCV. These results are all generally consistent with the mechanisms advanced by Trier and Davis (2002) and Davis and Trier (2002) for the development of heavy-rain-producing convection near an MCV.

4.3 *Surface features*

In contrast to most long-lived convective systems, this MCS was very slow in producing a low-

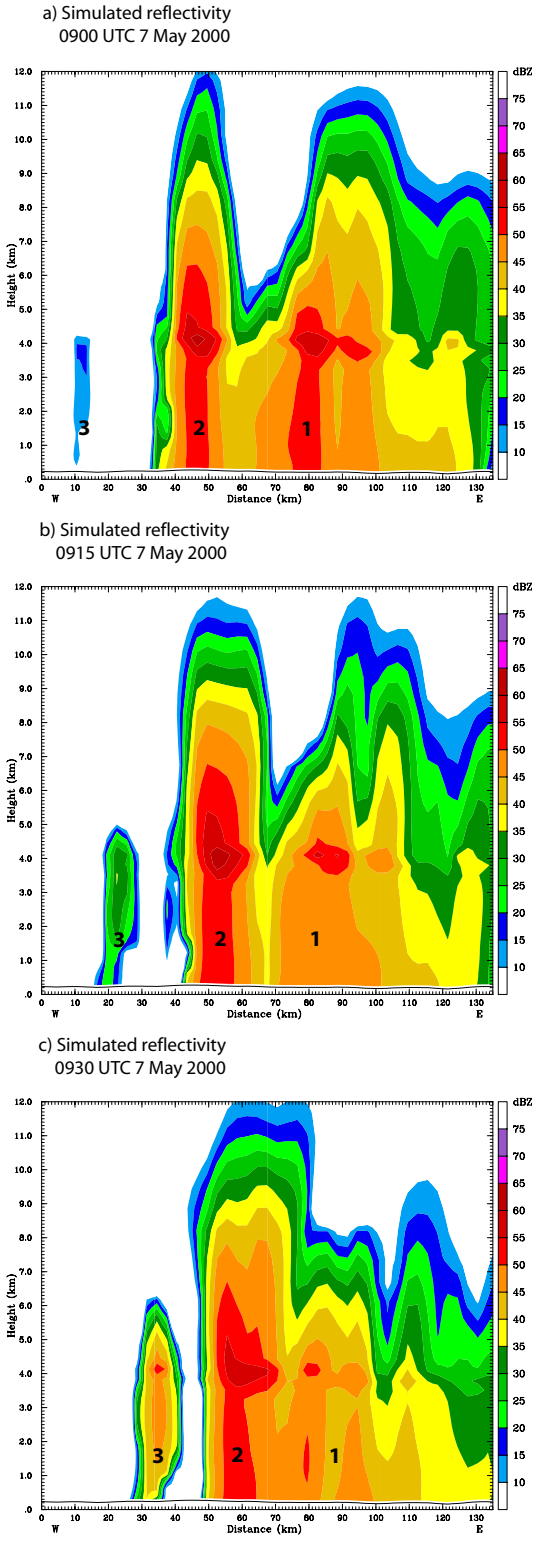

Figure 8: Cross-sections of simulated reflectivity at (a) 0900, (b) 0915, and (c) 0930 UTC 7 May through the line noted in Fig. 5b. Numbers refer to individual convective cells discussed in text.

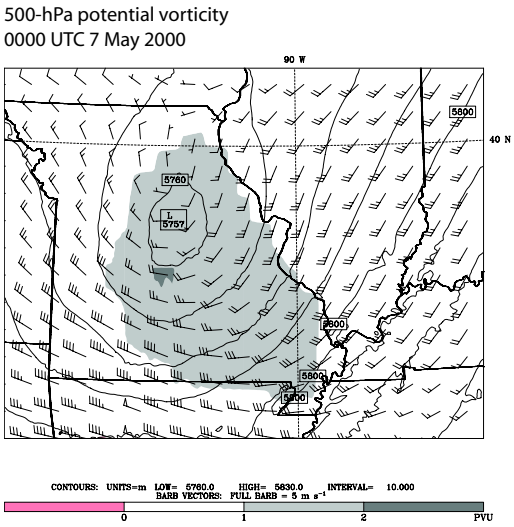

Figure 9: Potential vorticity (shaded, contours every 1 PVU), geopotential height (contoured every 10 m), and winds (long barb = 5 m s^{-1}) on domain 2 at 500 hPa for the model initial analysis at 0000 UTC 7 May 2000.

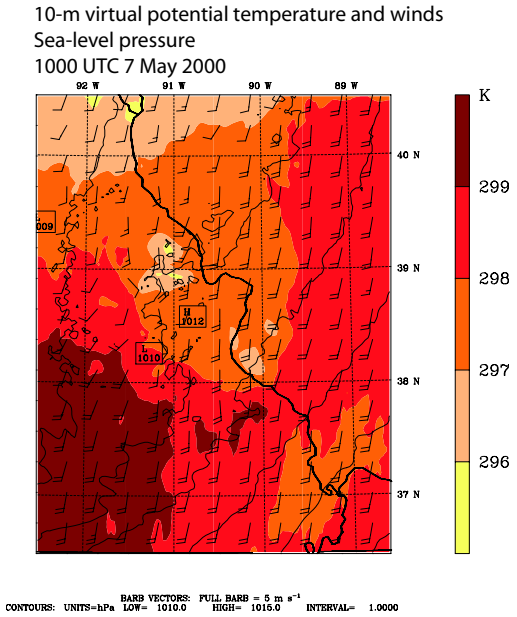

Figure 11: Virtual potential temperature at 10-m AGL (color contours every 1 K), sea-level pressure (contours every 1 hPa) and 10 m AGL winds at 1000 UTC 7 May 2000. Wind barbs are plotted at every tenth model grid point. The portion of domain 2 displayed is the same as that in Fig. 5.

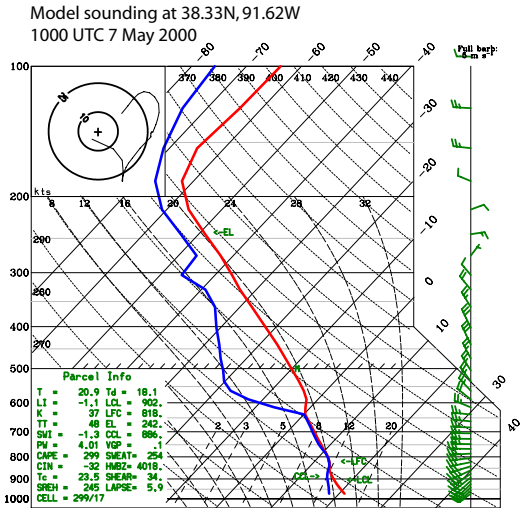

Figure 10: Model skew-T log p diagram from 1000 UTC 7 May 2000 at 38.33°N latitude, 91.62°W longitude (just west of the active convection).

level cold pool and outflow boundary. Convection repeatedly developed in certain areas for several hours before a discernable mesoscale outflow boundary was evident in the model output; by 1000 UTC, when the model had already produced over 200 mm of rain, the "cold pool" at the surface was only approximately 2 K cooler than the surrounding areas (Fig. 11). The divergence field near the surface at this time paints a similar picture, with only storm-scale maxima and minima in divergence at 1000 UTC (Fig. 12a). Finally, by 1200 UTC the convergence signature indicative of a mesoscale outflow boundary develops, though the convection begins to weaken only a few hours later (Fig. 12b). Again, while these features may not be well-resolved at a model grid spacing of 3 km, preliminary results with 1-km grid spacing show similar results.

The high relative humidity below 640 hPa (Fig. 10) in the vicinity of the convection limits the evaporation of raindrops and as such inhibits the development of a well-defined cold pool (while increasing the precipitation efficiency). While the absence of a strong cold pool certainly contributes to the slow system motion observed in this case, traditional theories for the maintenance of mesoscale deep convection (e.g., Rotunno et al. 1988) rely on the lifting provided by convectively-generated cold pools.

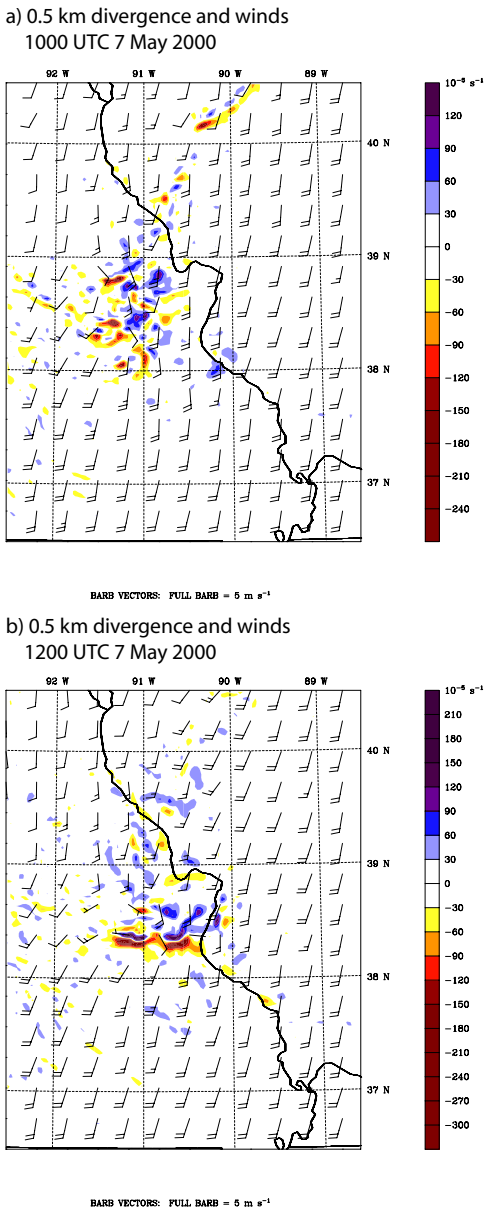

Figure 12: Divergence (color contours every $30\times$ 10^{-5} s^{-1}) and winds at 0.5 km AGL for (a) 1000 UTC and (b) 1200 UTC 7 May 2000. Wind barbs are plotted at every tenth model grid point.

However, in this case the convection is long-lived without the benefit of strong cold-pool lifting. It is unclear whether the mechanisms associated with the MCV and the weak cold pool are solely sufficient for maintaining the convection or whether other as yet unidentified mechanisms also play a role. Further work on this and other cases will investigate this issue further.

5. CONCLUSIONS

Results from WRF model simulations of the extreme-rain-producing MCS on 7 May 2000 are presented herein. The primary findings are summarized as follows:

- The WRF model, in a configuration with few modifications, is able to successfully replicate the backbuilding, quasistationary area of convection that occurred in this event. Though the precipitation forecast underestimated the observed rainfall amounts, many of the features of the convection were well represented.
- The effects of a mesoscale convective vortex on the convection in this event are generally consistent with mechanisms proposed in past observational and modeling studies.
- Despite the absence of a well-defined cold pool and outflow boundary, deep convection repeatedly develops and is maintained over east-central Missouri in the simulations.

Ongoing work is aimed at looking more closely at the mechanisms for initiating and maintaining backbuilding convection. In future efforts, it is hoped that long-lived quasi-stationary convection can be simulated in an idealized framework to further understand these difficult-to-predict systems that can produce extreme rainfall and have significant societal impacts.

6. ACKNOWLEDGEMENTS

WSR-88D data presented herein was obtained from the National Climatic Data Center. Computing resources were provided by the National Center for Atmospheric Research, which is sponsored by the National Science Foundation. The authors would like to thank Drs. Jason Knievel and George Bryan for discussions regarding this work and assistance in using the WRF model. This research was supported by National Science Foundation Grant ATM-0500061.

7. REFERENCES

Bryan, G. H. and J. M. Fritsch, 2000: Moist absolute instability: The sixth static stability state. *Bull. Amer. Meteor. Soc.*, **81**, 1207–1230.

Davis, C. A. and S. B. Trier, 2002: Cloud-resolving simulations of mesoscale vortex intensification and its effect on a serial mesoscale convective system. *Mon. Wea. Rev.*, **130**, 2839–2858.

Fritsch, J. M. and R. E. Carbone, 2004: Improving quantitative precipitation forecasts in the warm season: A USWRP research and development strategy. *Bull. Amer. Meteor. Soc.*, **85**, 955-965.

Gilmore, M. S. J. M. Straka, and E. N. Rasmussen, 2004: Precipitation uncertainty due to variations in precipitation particle parameters within a simple microphysics scheme. *Mon. Wea. Rev.*, **132**, 2610–2627.

Glass, F. H. J. P. Gagan, and J. T. Moore, 2001: The extreme east-central Missouri flash flood of 6–7 May 2000. Preprints, *Symp. on Precipitation Extremes: Prediction, Impacts, and Responses,* Albuquerque, NM, Amer. Meteor. Soc., 174–179.

Maddox, R. A., C. F. Chappell, and L. R. Hoxit, 1979: Synoptic and meso-α scale aspects of flash flood events. *Bull. Amer. Meteor. Soc.*, **60**, 115–123.

NOAA, cited 2005: Natural hazard statistics. [Available online at http://www.nws.noaa.gov/om/hazstats.shtml.]

Rotunno, R. J. B. Klemp, and M. L. Weisman, 1988: A theory for strong long-lived squall lines. *J. Atmos. Sci.*, **61**, 361–382.

Schumacher, R. S., and R. H. Johnson, 2005: Organization and environmental properties of extreme-rain-producing mesoscale convective systems. *Mon. Wea. Rev.*, **133**, 961–976.

Trier, S. B. C. A. Davis, and W. C. Skamarock, 2000: Long-lived mesoconvective vortices and their environment. Part II: Induced thermodynamic destabilization in idealized simulations. *Mon. Wea. Rev.*, **128**, 3396–3412.

Trier, S. B. and Davis, C. A. 2002: Influence of balanced motions on heavy precipitation within a long-lived convectively generated vortex. *Mon. Wea. Rev.*, **130**, 877–899.